JOPAT Vol 23(1), 1268 - 1292, January - June. 2024 Edition
ISSN2636 – 5448 https://dx.doi.org/10.4314/jopat.v23i1.7

Biochemical Reactivity and Inhibiting Studies on cyclopentane-anthraquinone based compounds as Potential Vascular endothelial growth factor Inhibitors

Oyebamiji Abel K. [1,5*], Akintelu Sunday A.[2], Akintayo Emmanuel T.[3], Babalola Jonathan O.[1,4]

[1]Industrial Chemistry Programme, Bowen University, PMB 284, Iwo, Osun State, Nigeria.
[2]School of Chemistry and Chemical Engineering, Beijing Institute of Technology, Beijing 100811, China.
[3]Department of Chemistry, Ekiti State University, Ado-Ekiti, Nigeria.
[4]Department of Chemistry, University of Ibadan, Ibadan, Nigeria.
[5]Good Health and Wellbeing Research Clusters (SDG 03), Bowen University, PMB 284, Iwo, Nigeria.

Abstract:

Introduction: The efficiency of heterocyclic compounds as potential vascular endothelial growth factor inhibitor has drawn the attention of scientists globally.

Objective of study: this work is aimed at identifying the most proficient anticancer cyclopentane-anthraquinone based compound via density functional theory and molecular modeling analysis.

Method: In this work, the inhibiting capacities of cyclopentane-anthraquinone based compounds were examined using *insilico* method. The optimization was carried out using density functional theory and the molecular modeling studies were executed via induce fit docking and molecular dynamics simulation methods.

Result: Compound 13 among other compounds have highest binding affinity compared to 5-FU (Standard) via induce fit docking study; however, the report by binding energy, root mean square deviation and root mean square fluctuation via molecular dynamic simulation study revealed otherwise. The pharmacokinetic study on compound 13 and 5-FU was examined and reported. **Conclusion**: These discoveries may provide perception into developing more potent potential library of drug-like triazole-based compounds as proficient anti-diabetic agents.

Keywords: cancer; anthraquinone; Ligands; Residues, *In silico*; Scoring

Correspondence: *Email: abel.oyebamiji@bowen.edu.ng

Introduction

Cancer remains an unrestrained multiplication of cells and the establishment of initial stage of tumor which possess the ability to negatively affect neighboring nerves [1, 2]. According to report by Karatoprak *et al*., 2022, it was described as an irregularity which exists in cell configuration due to chromosomal modifications [3]. Globally, cancer has been rated to be second in position among other ailments which cause mortality and this has been observed to be a function of speed and energetic advance processes in human body system [4]. In cancer study, several positive advances have been recorded, but, resistance to potential anti-cancer agents observed in many cancer patients have been described to diminish the feat of this advancements [5, 6]; thus, the need for efficient and reliable anticancer agent is vital so as to give lasting solution to this menace.

Vascular endothelial growth factor has been reported by many scientists to play a crucial part in the formation of blood container [7, 8]. According to Iraj *et al*., 2023, VEGF has series of sub categories such VEGF-A, VEGF-B, VEGF-C, VEGFD, VEGFE, VEGF-F as well as placental growth factor [9] and report have shown that VEGF family comprises of eight cysteine residues and all these residues are sealed at static spot that are associated to PDGF family [10]. Also, this enzyme has the ability to act as controlling agent of this vital process. It comprises of various chemical compounds with special tasks. Promotion of endothelial cell development, movement and subsistence from original blood vessels has been attributed to instigating VEGF which prompts a system of signaling practices [11, 12].

The reports on biological activities of heterocycles have confirmed the proficiency of heterocyclic compounds [13]. Combination of compounds such as cyclopentane-anthraquinone based compounds consists of cyclopentane and anthraquinone. These sets of compounds have been reported to be biologically active as antitumor, anti-diabetic and antioxidant agents [14-16]. Thus, this work is aimed at identifying the most proficient anticancer cyclopentane-anthraquinone based compound via density functional theory and molecular modeling analysis.

Methodology

Ligand and Receptor Preparation

The studied ligands [17] (table 1) were modeled in a 2-dimensional format using ChemDraw (level: professional; version: 22.2.0.3300) [18] and the modeled compounds were transformed into 3-dimensional format which were further optimized using Spartan 14 software [19]. Several factors in different segments were considered for the calculation of the studied compounds such as Calculate (equilibrium geometry at ground state with density functional via 6-31G** as basis set in vacuum). Also, the calculation started from current geometry and the total charge was observed to be neutral with unpaired electron which was also zero. The duration for the completion of optimization was observed to be due to atoms in the heterocycles, the bond involved, the method used for calculation as well as the basis set used. The features obtained from the optimized compounds were obtained and presented for further study.

Vascular endothelial growth factor (pdb id: 2vpf) [20] was retrieved from protein data bank and the studied protein sequence was edited using sequence editor (an embedded tool in molecular operating environment software) before subjecting it to Quickprep tool for treating and preparing the studied protein structure. The binding site was located using site finder and five (5) binding sites were predicted. The factors considered for each predicted site were propensity for ligand binding (PLB), size, hydrophobic regions, sides, as well as the amino acid residues (Table 2). The treated and prepared protein structure was saved in .moe format before docking calculation using induced fit method. The obtained results from docked complexes were presented in kcal/mol and the types of interactions involved in the docked complexes were displayed and reported.

Molecular Dynamic Simulation Analysis

Compound 13- vascular endothelial growth factor complex and 5-Fluorouracil-vascular endothelial growth factor complex were selected for molecular dynamic simulation study. Compound 13 was selected as the compound with highest binding affinity among all the studied compounds while 5-Fluorouracil served as the reference compound. The parameterization for the selected compounds was accomplished via Swissparam software

(https://www.swissparam.ch/)_[21] and diverse formats were obtained. In this study, appropriate force field (Charmm36m) in Gromacs software [22, 23] was chosen for simulation. Also, suitable quantity of water molecules was added to the simulating system so as to accomplish solvation. More so, proper ions were added at persistent pressure and temperature. The final simulation was executed via 100nanoseconds and the obtained results were reported accordingly.

Calculation of Pharmacokinetic Properties of Selected Compounds

The features obtained for Lipinski rule of five and other pharmacokinetic properties for compound 13 and the referenced compounds were observed and reported. ADMETSar 1 [24] was employed to execute this analysis and the reported results were presented appropriately.

Table 1: Two dimensional structure of the studied cyclopentane-anthraquinone based compounds

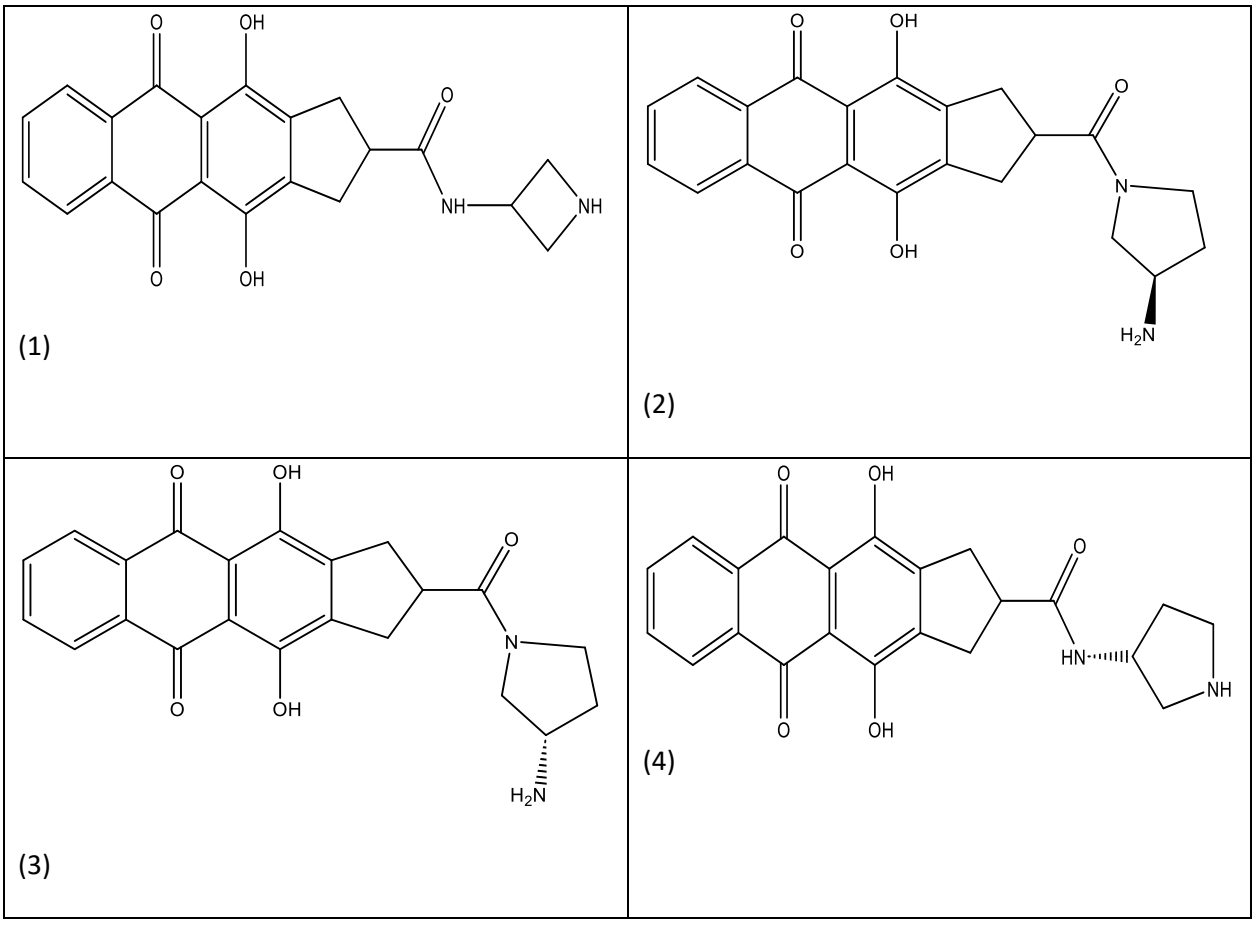

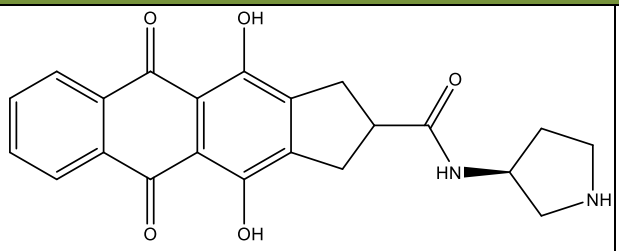

(5)

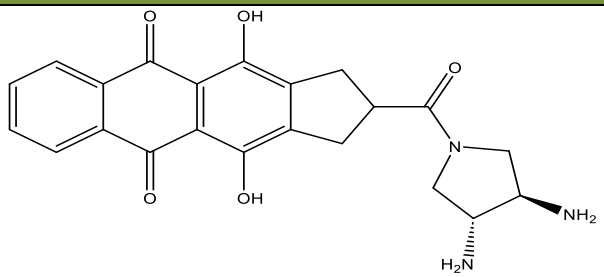

(6)

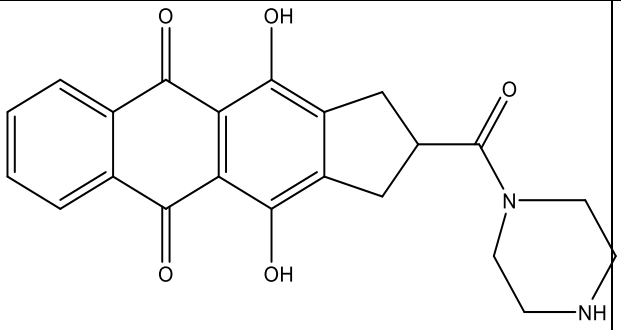

(7)

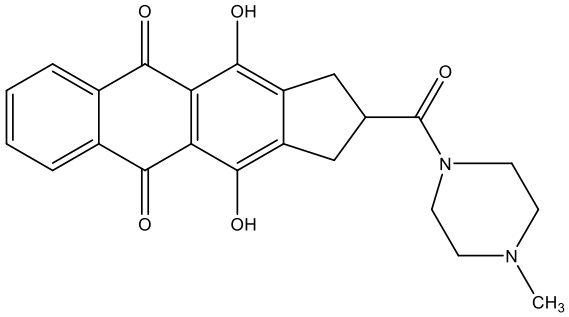

(8)

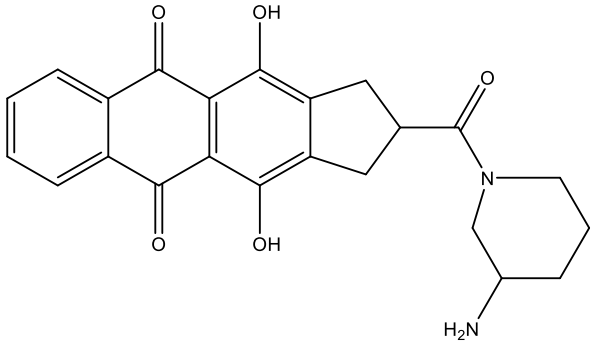

(9)

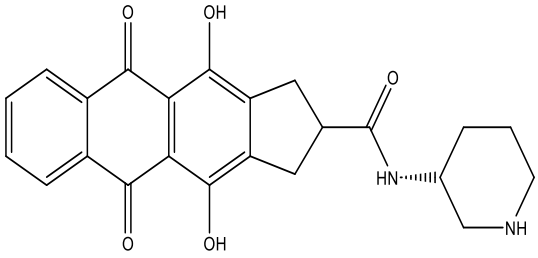

(10)

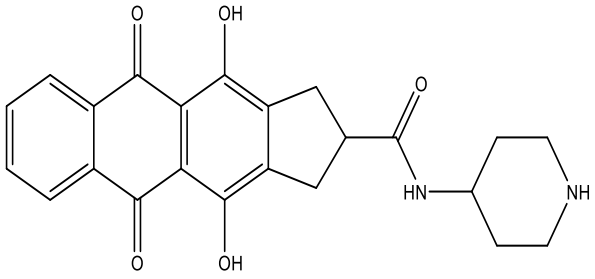

(11)

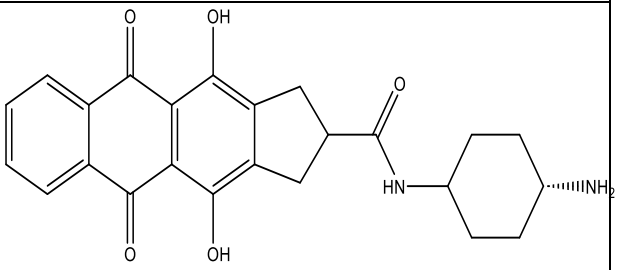

(12)

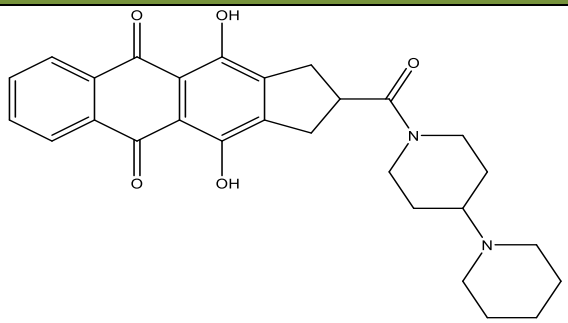

(13)

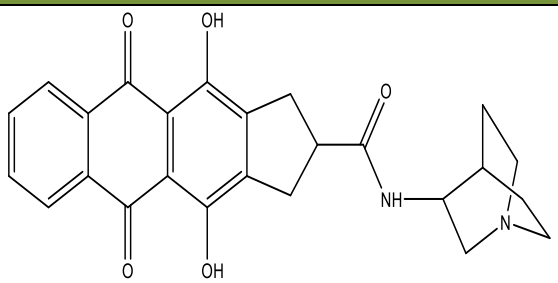

(14)

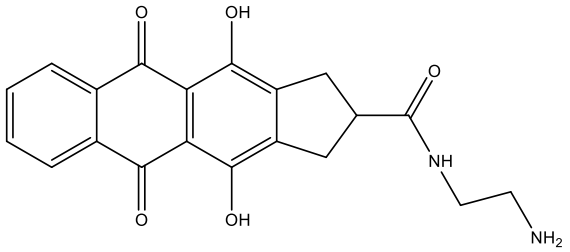

(15)

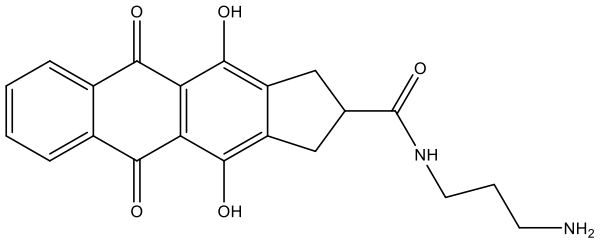

(16)

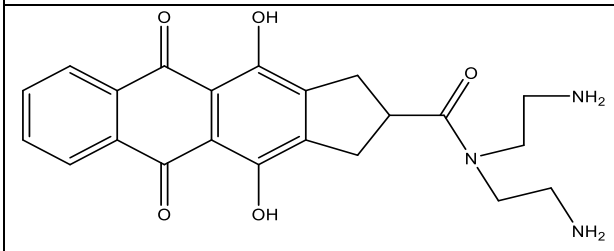

(17)

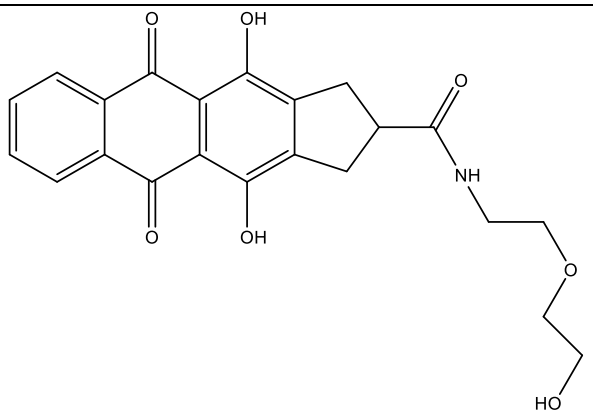

(18)

Table 2: Predicted binding sites obtained from Tyrosine Phosphatase-L1

Site	Size	PLB	Hyd	Side	Residues
1	22	1.95	16	20	1:(ASP34 ILE35 PHE36 GLU42 ILE43 TYR45 ILE46 PHE47 SER50)
2	7	-0.22	9	17	1:(GLU38 TYR39 ARG56 ASN75 SER95 PHE96 LEU97)
3	19	-0.24	2	6	1:(GLY59 CYS60 CYS61 ASN62 ASP63 GLU64 LEU66 GLU67 CYS68)
4	3	-0.70	2	4	1:(ARG23 SER24 HIS27 ILE29)
5	11	-0.78	6	11	1:(THR71 LYS101 CYS102 GLU103)

Results and Discussion

Structural Features for studied compounds

The potential reactivity of cyclopentane-anthraquinone based compounds could be attributed to the calculated features obtained from the optimized studied compounds. According to Semire *et al*., 2012, [25] any chemical compound with highest HOMO energy value stands a chance of reacting better than other studied compounds while molecule with lowest LUMO value have highest tendency to receive electron which thereby increase it chance of reacting better than other studied compounds. Therefore, compound **13** have highest HOMO value and 1,4'-bipiperidine as derivative attached to the parent compound proved to have enhanced the reactivity and donating of electron of compound **13**. Also, compound **4** and **18** with lowest LUMO value proved to have a potential ability to react well than other studied ligands and this claim was in agreement with the work carried out by Waziri *et al*., 2024 [26].

More so, the report by Abdulazeez *et al*., 2016 and Pegu *et al*., 2017, [27, 28] revealed that energy gap exposes the reactivity and stability indices of any compounds. Also, the spectroscopic features of any studied complexes intensely rely on it calculated energy gap. According to Migahed *et al*., 2016 [29] optimized ligand with lowest energy gap have every tendency to be polarized effortlessly and react well than other studied compounds; therefore, compound 13 possess ability to be softer and react with receptor/neighboring compounds than other compounds under study (Table 3). The calculated Lipophilicity (log p) for all the studied compounds were ≤ 5 which was set to be the standard for calculated log p [30]. This showed that all the studied compounds have the ability to act as drug agent. Also, table 3 showed other calculated features obtained from the optimized studied compounds.

Table 3: Calculated Features from the optimized cyclopentane-anthraquinone based compounds

	E_H	E_L	EGap	DM	Mol Wei	Polar Sur. Area	Ovality	LOG P
1	-5.90	-2.91	2.99	4.67	378.384	94.502	1.51	-2.08
2	-5.81	-2.83	2.98	3.23	392.411	95.491	1.51	-2.09
3	-5.80	-2.82	2.98	2.91	392.411	95.602	1.51	-2.09
4	-5.88	-2.92	2.96	4.48	392.411	92.773	1.52	-1.80
5	-5.84	-2.85	2.99	3.26	392.411	92.752	1.52	-1.80
6	-5.77	-2.80	2.97	3.07	407.426	120.048	1.53	-3.28
7	-5.84	-2.85	2.99	3.55	392.411	83.231	1.50	-1.83
8	-5.84	-2.85	2.99	3.54	406.438	73.152	1.52	-1.45
9	-5.86	-2.88	2.98	3.60	406.438	95.141	1.52	-1.81
10	-5.88	-2.89	2.99	4.50	406.438	92.447	1.54	-1.52
11	-5.87	-2.88	2.99	2.79	406.438	92.404	1.54	-1.52

12	-5.88	-2.89	2.99	3.25	420.465	104.431	1.57	-1.50
13	-5.70	-2.85	2.85	4.03	474.557	72.790	1.60	-0.18
14	-5.77	-2.89	2.88	3.05	432.476	82.993	1.55	-1.26
15	-5.89	-2.91	2.98	4.00	366.373	105.520	1.51	-2.34
16	-5.89	-2.90	2.99	4.53	380.400	105.456	1.54	-2.06
17	-5.89	-2.90	2.99	3.63	409.442	120.592	1.57	-3.00
18	-5.91	-2.92	2.99	3.70	411.410	108.437	1.57	-2.11

Induced fit Molecular Docking Analysis

Eighteen cyclopentane-anthraquinone based compounds were docked against vascular endothelial growth factor (pdb id: 2vpf) and the calculated binding affinity as well as the amino acid residues and the involved types of nonbonding interaction were reported in Table 4. According to Ruddarraju *et al*., 2016, [31] induced fit molecular docking study predicts the inhibiting proficiency of chemical compounds. As shown in table 4, different scoring values as well as predicted amino acid residues with various types of interactions were observed for docked compound 1-18. The calculated scoring value for individual studied docked complex was compared with the scoring of the docked reference compound.

The calculated binding affinity was -5.4552393 kcal/mol for compound **1**, -5.67925215 kcal/mol compound **2**, -5.63414669 kcal/mol compound **3**, -5.67842102 kcal/mol compound **4,** -5.70559978 kcal/mol compound **5**, -5.67465687 kcal/mol compound **6**, -5.61930895 kcal/mol compound **7** -5.62658787 kcal/mol compound **8,** -5.58630705 kcal/mol compound **9**, -5.64910364 kcal/mol compound **10**, -5.92183352 kcal/mol compound **11**, -5.73948622 kcal/mol compound **12**, -6.19048309 kcal/mol compound **13**, -5.69344139 kcal/mol for compound **14**, -5.32146502 kcal/mol for compound **15**, -5.65927029 kcal/mol for compound **16**, -5.65706158 kcal/mol for compound **17**, and -5.90476322 kcal/mol for compound **18**. According to Morakinyo *et al*., 2024, the lower the calculated binding affinity value, the stronger the ability of the molecule to inhibit the target [32]; therefore, compound 13 with lowest scoring value have the greatest tendency to inhibit vascular endothelia growth factor. This was in agreement with the report by Oyebamiji *et al*., 2024 [33] that compound with lowest scoring value have highest chance of inhibiting the target; thus compound 13 was predicted to have capability to inhibit the target better than other studied cyclopentane-anthraquinone based compounds and the referenced compound.

More so, the amino acid as well as the non-bonding interactions present in the docked complexes were CYS 102 (H-acceptor) for compound **1**-2vpf complex (Figure 1); VAL 69 (pi-H) for compound **2**-2vpf complex (Figure 2); CYS 102 (H-acceptor) for compound **3**-2vpf complex (Figure 3); CYS 104 (H-acceptor), CYS

102, H-acceptor for compound **4**-2vpf complex (Figure 4); CYS 57 (H-donor), CYS 68 (H-acceptor), CYS 60 (pi-H) for compound **6**-2vpf complex (Figure 6); LEU 97 (H-acceptor) for compound **7**-2vpf complex (Figure 7); GLY 59 (H-donor), GLU 67 (pi-H), GLU 67 (pi-H) for compound 8-2vpf complex (Figure 8); CYS 102 (H-acceptor) for compound **9**-2vpf complex (Figure 9); HIS 27 (H-pi) compound **10**-2vpf complex (Figure 10); LEU 97 (H-acceptor) for compound **12**-2vpf complex (Figure 12); GLN 22 (H-acceptor), HIS 27 (H-pi), TYR 25 (pi-pi) for compound **13**-2vpf complex (Figure 13); CYS 104 (H-donor), CYS 26 (H-donor), CYS 104 (H-acceptor), CYS 102 (H-acceptor) for compound **15**-2vpf complex (Figure 15); ARG 23 (H-donor), CYS 102 (H-acceptor), HIS 27 (H-pi) for compound **16**-2vpf complex (Figure 16); GLN 22 (H-acceptor) for compound **17**-2vpf complex (Figure 17); CYS 61 (H-donor), CYS 68 (H-acceptor) for compound **18**-2vpf complex (Figure 18).

As shown in table 4, no non-bonding interaction was observed in compound **5**-2vpf complex, compound **11**-2vpf complex and compound **14**-2vpf complex and this was pictorially presented in figure 4, 11, and 14

Table 4: Calculated scoring in kcal/mol and the predicted interactions

	Scoring (kcal/mol)	Amino Acid Residues and Interactions
1	-5.4552393	CYS 102 (A); H-acceptor
2	-5.67925215	VAL 69 (A) pi-H
3	-5.63414669	CYS 102 (A) H-acceptor
4	-5.67842102	CYS 104 (A) H-acceptor; CYS 102 (A) H-acceptor
5	-5.70559978	-
6	-5.67465687	CYS 57 (A) H-donor ; CYS 68 (A) H-acceptor; CYS 60 (A) pi-H
7	-5.61930895	LEU 97 (A) H-acceptor
8	-5.62658787	GLY 59 (A) H-donor; GLU 67 (A) pi-H; GLU 67 (A) pi-H
9	-5.58630705	CYS 102 (A) H-acceptor
10	-5.64910364	HIS 27 (A) H-pi
11	-5.92183352	-
12	-5.73948622	LEU 97 (A) H-acceptor
13	-6.19048309	GLN 22 (A) H-acceptor; HIS 27 (A) H-pi; TYR 25 (A) pi-pi
14	-5.69344139	-
15	-5.32146502	CYS 104 (A) H-donor; CYS 26 (A) H-donor; CYS 104 (A) H-acceptor ; CYS 102 (A) H-acceptor
16	-5.65927029	ARG 23 (A) H-donor; CYS 102 (A) H-acceptor; HIS 27 (A) H-pi
17	-5.65706158	GLN 22 (A) H-acceptor
18	-5.90476322	CYS 61 (A) H-donor; CYS 68 (A) H-acceptor
Ref (5-FU)	-4.06899166	-

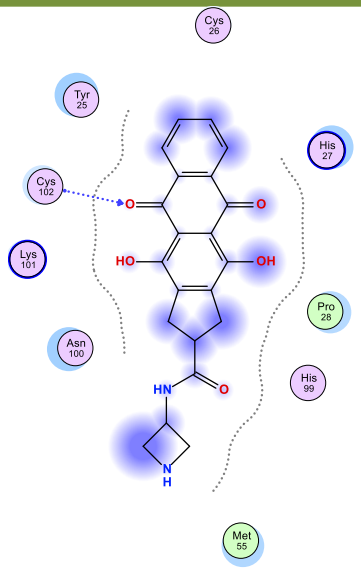

Figure 1: 2D structure of docked compound **1**-2vpf complex

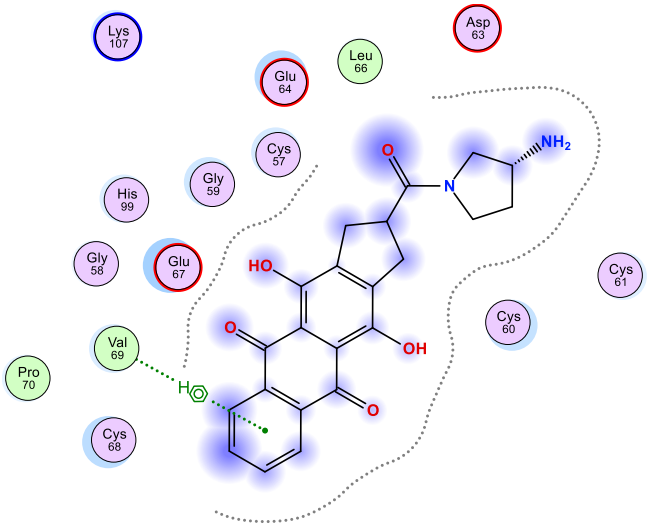

Figure 2: 2D structure of docked compound 2-2vpf complex

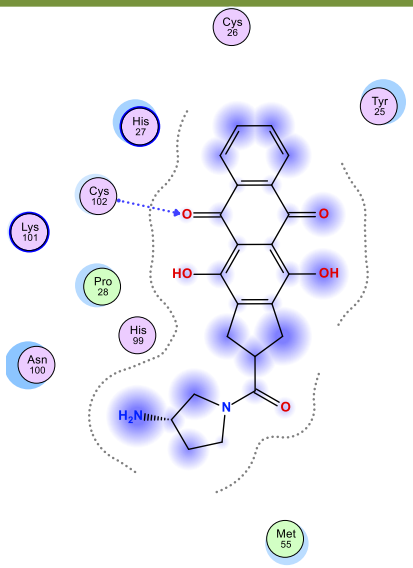

Figure 3: 2D structure of docked compound 3-2vpf complex

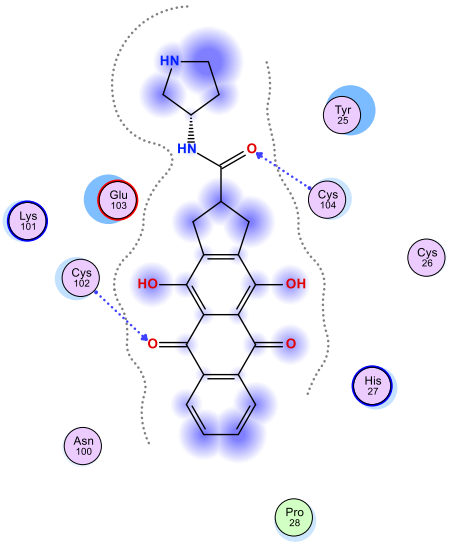

Figure 4: 2D structure of docked compound 4-2vpf complex

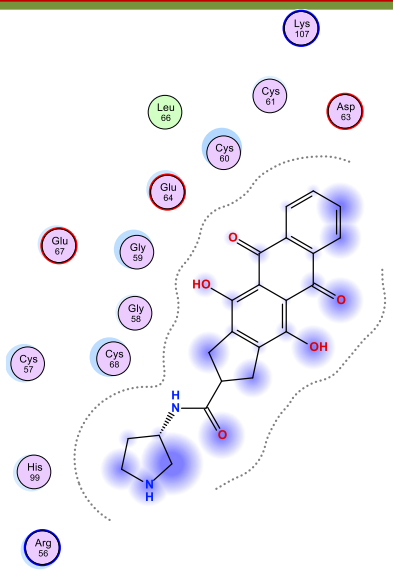

Figure 5: 2D structure of docked compound 5-2vpf complex

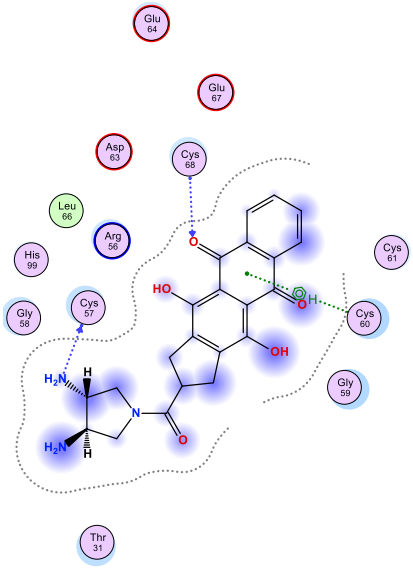

Figure 6: 2D structure of docked compound **6**-2vpf complex

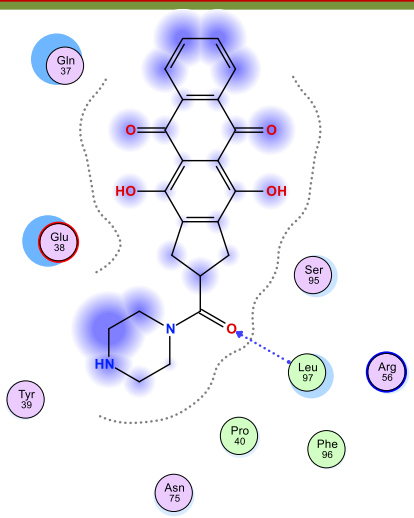

Figure 7 : 2D structure of docked compound 7-2vpf complex

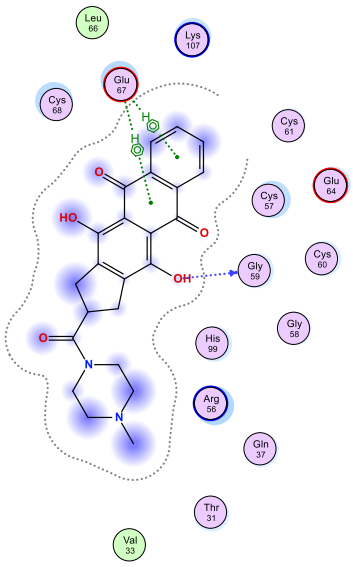

Figure 8: 2D structure of docked compound 8-2vpf complex

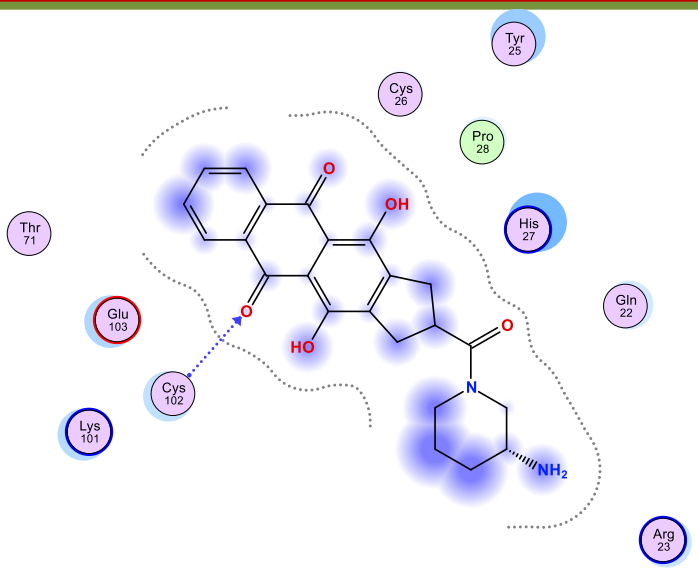

Figure 9: 2D structure of docked compound **9**-2vpf complex

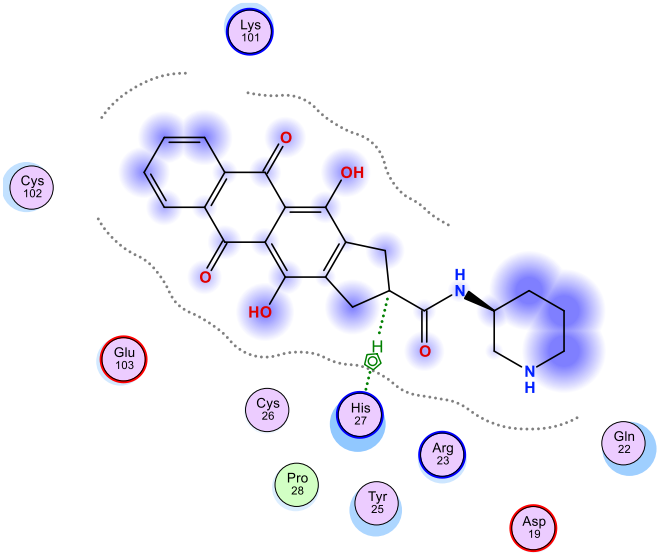

Figure 10: 2D structure of docked compound **10**-2vpf complex

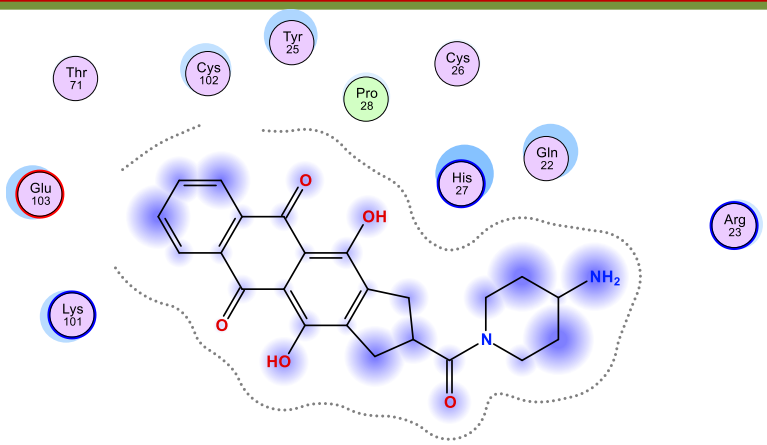

Figure 11: 2D structure of docked compound **11**-2vpf complex

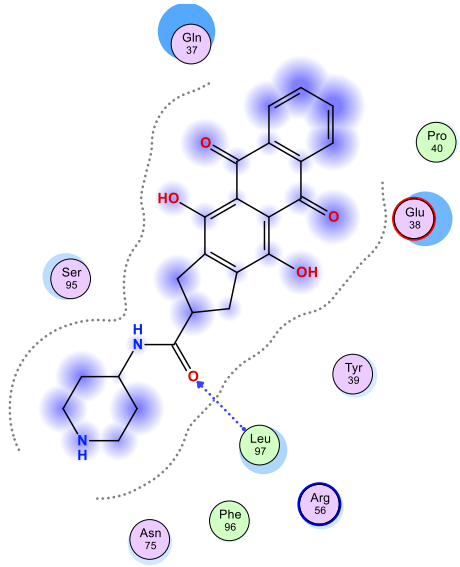

Figure 12: 2D structure of docked compound **12**-2vpf complex

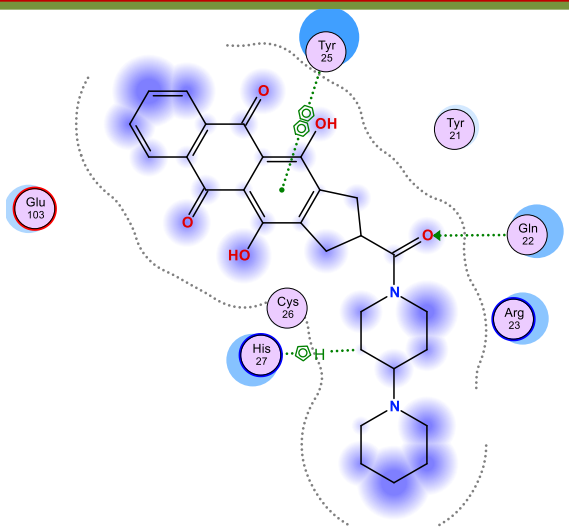

Figure 13: 2D structure of docked compound **13**-2vpf complex

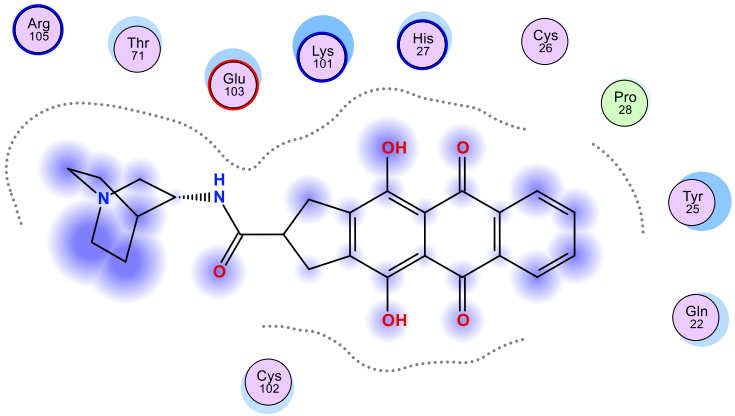

Figure 14: 2D structure of docked compound **14**-2vpf complex

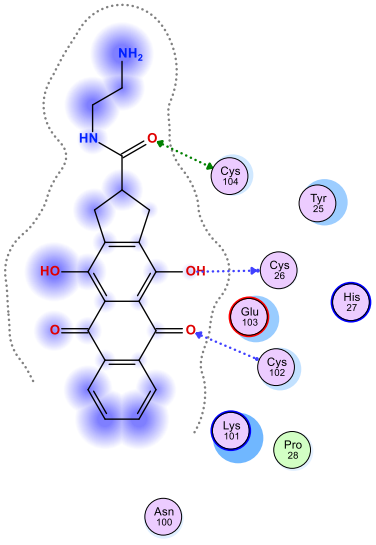

Figure 15: 2D structure of docked compound **15**-2vpf complex

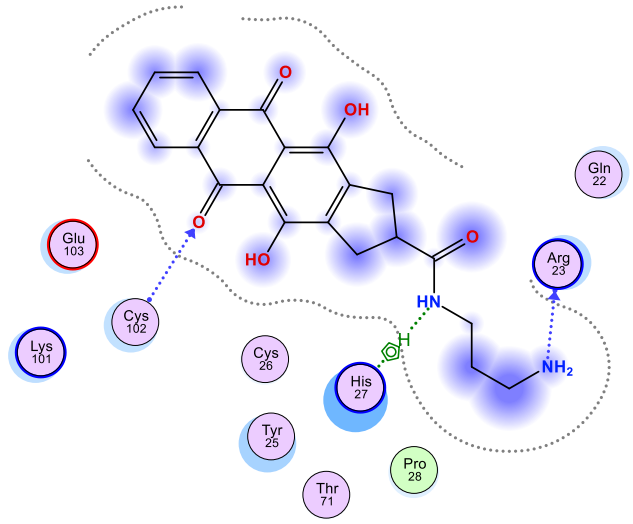

Figure 16: 2D structure of docked compound **16**-2vpf complex

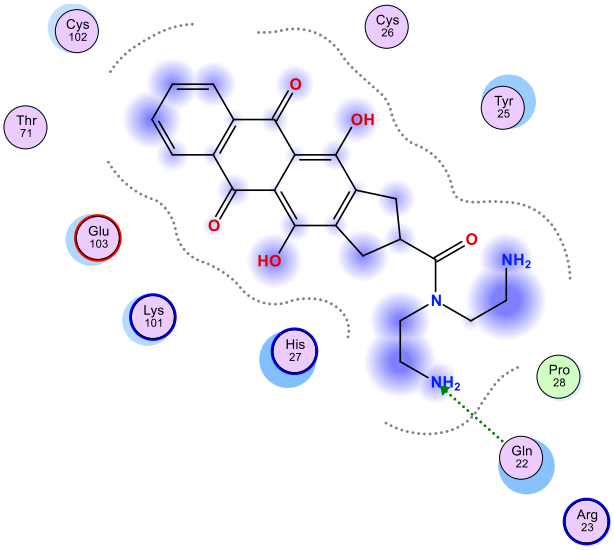

Figure 17: 2D structure of docked compound **17**-2vpf complex

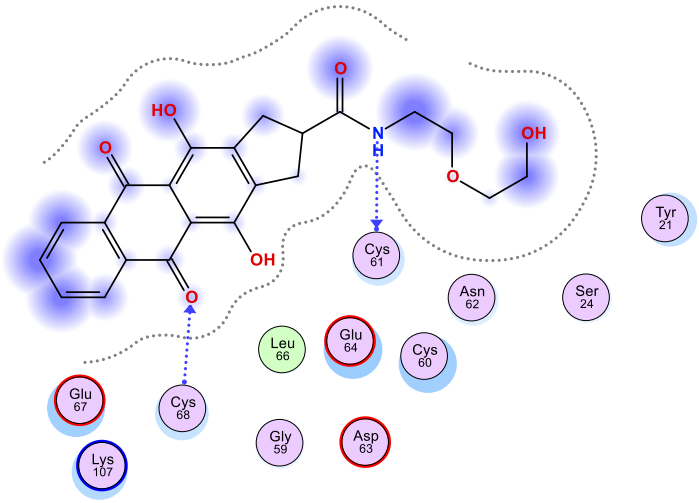

Figure 18: 2D structure of docked compound 18-2vpf complex

Molecular Dynamic Simulation Study

In this work, three sections (Root mean square deviation (RMSD), root mean square fluctuation (RMSF) and actual binding energies for the studied complexes) were considered and reported on the compound with highest binding affinity and compared with the referenced compound. In this work, the actual inhibiting potency of compound 13 against the studied receptor (pdb id: 2vpf) was revealed and compared to the inhibiting ability of the 5-FU. The claim about the highest inhibiting tendency of compound 13 against the studied target via predicted binding affinity was proved to be otherwise via the studied molecular dynamic simulation study. As shown in table 8, solvation free energy (ΔG_{sol}) was observed to support the calculated result for the 5-FU, while van der Waals free and ΔG_{gas} energies supported the calculated result for compound 13. However, the 5-FU with 3.16kcal/mol has highest binding energy than the predicted binding energy for compound 13 and this revealed that the standard molecule can act as potential inhibitor of the investigated target (pdb id: 2vpf) than compound 13. This report was supported by the predicted root mean square deviation and root mean square fluctuation (Figure 19 and 20).

Table 8: Binding Energy Components

	Binding Energy Components (kcal/mol)				
Complexes	**ΔE_{vdw}**	**ΔE_{ele}**	**ΔG_{gas}**	**ΔG_{sol}**	**ΔG_{bind}**
Comp13-2vpf	-15.08± 0.54	11.59± 0.7	-3.49± 0.86	12.81± 1.17	9.33± 0.48

REF-2vpf	-4.77±0.39	115.54 ±1.29	110.76 ±1.01	-107.6 ± 1.26	3.16 ±0.85

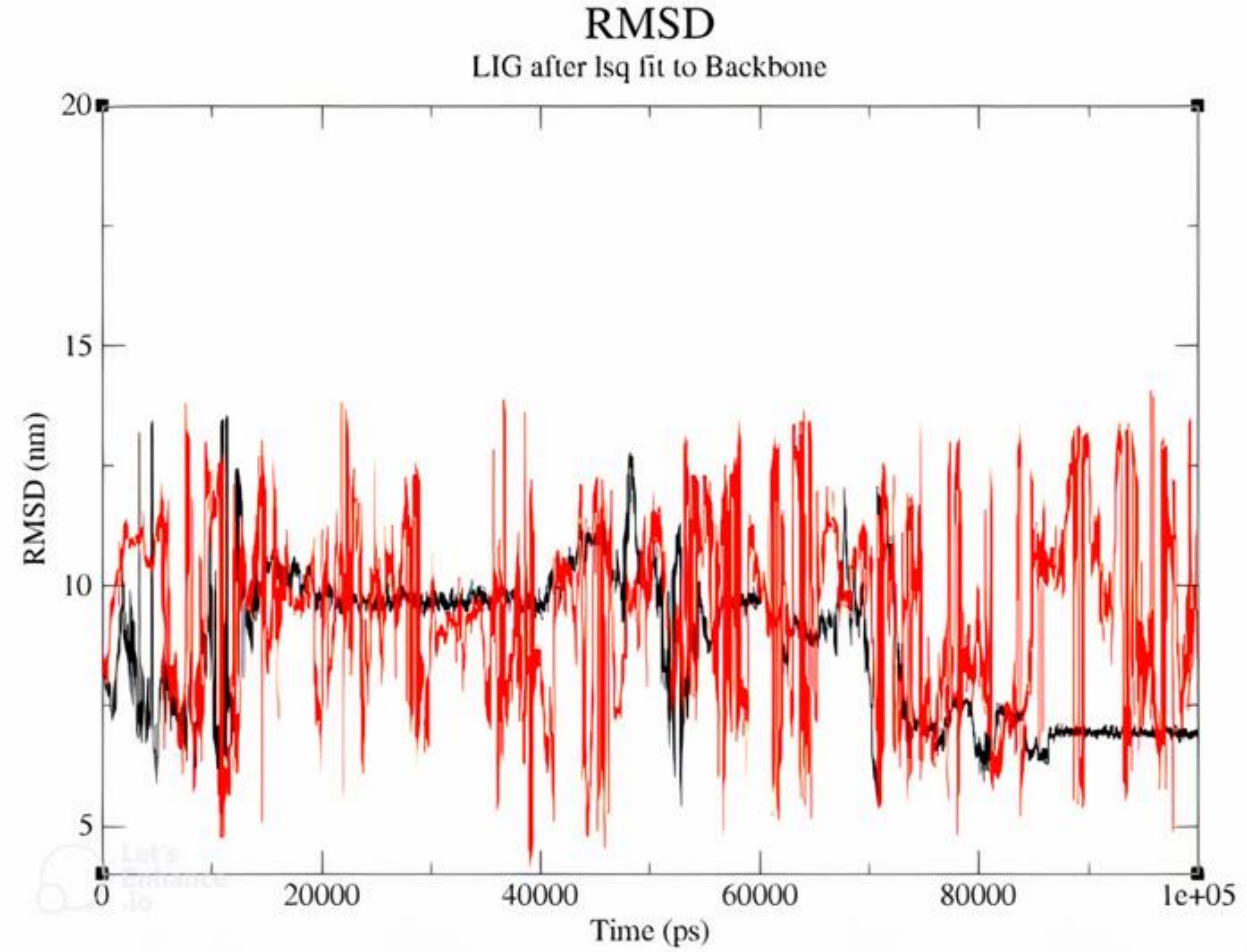

Figure 19: Predicted RMSD for compound 13-2vpf and 5-2vpf

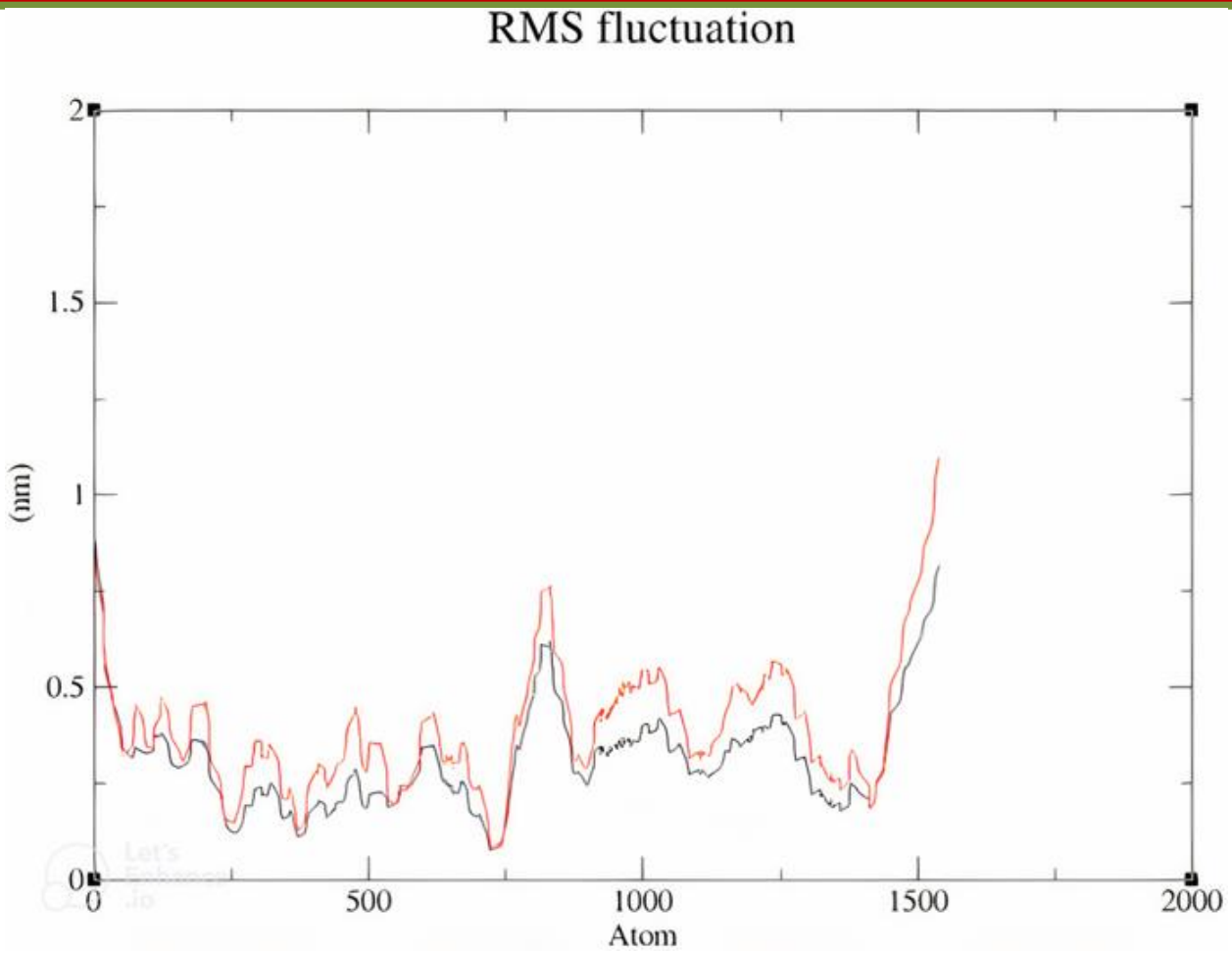

Figure 20: Predicted RMSD for 5-FU-2vpf and 5-2vpf

Pharmacokinetics Study

In this work, six features were observed to investigate absorptive capability of the studied compounds. The factors were blood-brain barrier, human intestinal absorption, Caco-2 permeability, p-glycoprotein substrate, p-glycoprotein inhibitor and renal organic cation transporter. The report by Kalantzi *et al.,* 2006 [34] showed that any calculated human intestinal absorption value (calculated in %) below 30% signifies a low level of absorption in human system; thus, the calculated values for human intestinal absorption for the compound 13 and 5-FU were above 30% and the is proved that they both have good absorption rate. Thus, as shown in supplementary table 1 and 2, compound 13 has higher absorption rate than 5-FU.

The predicted value for blood-brain barrier for compound 13 and 5-FU were 0.8671 and 0.9832 and this proved to be better since the predicted values were higher than 0.3. The predicted value for the selected compounds (0.7898 and 0.6609) for subcellular localization which described the distribution within human system prove to be good and they were observed to be higher than the referenced compound which agreed with the result reported by Speciale *et al*., 2021 [35]. As shown in supplementary table 1

and 2 the distributing capability of compound 13 was observed to be higher than 5-FU. In drug design, toxicity index is crucial and AMES toxicity was considered for compound 13 and referenced compound; thus, compound 13 is non-toxic while reference compound proved to be toxic as presented in supplementary table 1 and 2 [36-39]. Other factors considered were obtained and reported accordingly.

Conclusion

Cyclopentane-anthraquinone based compounds were studied using density functional theory method, molecular modeling approach and pharmacokinetics study. The features obtained from the optimized compounds revealed the reactivity of these compounds. Compound 13 proved to have highest ability to donate electron to the nearest compound as well as greatest ability to react well which were confirmed via highest HOMO and lowest energy gap. Also, the docking study revealed the ability of compound 13 (-6.19048309 kcal/mol) to inhibit vascular endothelial growth factor (pdb id: 2vpf) than other studied compounds as well as 5-FU (-4.06899166 kcal/mol). The 1,4'-bipiperidine attached to the parent compound was observed to have enhanced the biological activity and reactivity of compound 13. The actual binding energy components for compound 13-2vpf complex and 5-FU-2vpf complex validated the inhibiting capability of compound 13 and 5-FU against VEGF.

References

[1]. Siegel, R.L., Miller, K.D., Fuchs, H.E., Jemal, A. (2022) Cancer statistics, 2022, CA Cancer J. Clin. 72; 7. https://doi.org/10.3322/caac.21708.

[2]. Rivankar, S. (2014). An overview of doxorubicin formulations in cancer therapy, J. Cancer Res. Ther. 10; 853. https://doi.org/10.4103/0973-1482.139267.

[3]. Karatoprak, G.Ş., Akkol, E.K., Yücel, Ç., Acıkara, Ö.B., and Sobarzo-Sánchez, E. (2022). Oxidative Medicine and Cellular Longevity, Volume 2022, Article ID 7928200, 20 pages.

[4]. Emami, S. and Dadashpour, S. (2015). Current developments of coumarin-based anti-cancer agents in medicinal chemistry, European Journal of Medicinal Chemistry, 102; 611–630.

[5]. Kuete, V., Saeed, M. E., Kadioglu, O., et al., (2015). Pharmacogenomic and molecular docking studies on the cytotoxicity of the natural steroid wortmannin against multidrug-resistant tumor cells, Phytomedicine, 22(1); 120–127.

[6]. Olgen, S. (2018). Overview on anticancer drug design and development," Current Medicinal Chemistry, 25(15); 1704–1719.

[7]. Holmes, D.I., Zachary, I. (2005). The vascular endothelial growth factor (VEGF) family: angiogenic factors in

health and disease. *Genome Biol* 6: 209 https://doi.org/10.1186/gb-2005-6-2-209

[8]. Hicklin, D.J. and Ellis, L.M. (2005). Role of the Vascular Endothelial Growth Factor Pathway in Tumor Growth and Angiogenesis. Journal of Clinical Oncology, 23(5).

[9]. Iraj, A., Peter, J., Attya, B. (2023). Association analysis of Vascular Endothelial Growth Factor-A (VEGF-A) polymorphism in rheumatoid arthritis using computational approaches. Scientific Reports, 13: 21957

[10]. Shibuya, M. (2011). Vascular Endothelial Growth Factor (VEGF) and Its Receptor (VEGFR) signaling in angiogenesis: A crucial target for anti- and pro-angiogenic therapies. Genes Cancer 2(12), 1097–1105. https:// doi. org/ 10. 1177/ 19476 01911 423031

[11]. Shibuya, M. (2011). Vascular Endothelial Growth Factor (VEGF) and Its Receptor (VEGFR) Signaling in Angiogenesis: A Crucial Target for Anti- and Pro-Angiogenic Therapies. *Genes & Cancer*. 2(12): 1097-1105. doi:10.1177/1947601911423031

[12]. Tirronen, A., Downes, N.L., Huusko, J., Laakkonen, J.P., Tuomainen, T., Tavi, P., Hedman, M., Ylä-Herttuala, S. (2021**)**. The Ablation of VEGFR-1 Signaling Promotes Pressure Overload-Induced Cardiac Dysfunction and Sudden Death. *Biomolecules*, 11: 452. https://doi.org/10.3390/biom11030452.

[13]. Oyebamiji, A.K., Fadare, O.A., Semire, B. (2020). Anti-gastric cancer activity of 1,2,3-triazolo[4,5-d]pyrimidine hybrids (1,2,3-TPH): QSAR and molecular docking approaches. Heliyon 6: e03561.

[14]. Ming-Xia, S., Xian-Qing, D. (2018). Recent developments on triazole nucleus in anticonvulsant compounds: a review, J. Enzym. Inhib. Med. Chem. 33 (1): 453–478.

[15]. Mavrova, A.T., Wesselinova, D., Tsenov, J.A., Lubenov, L.A. (2014) Synthesis and antiproliferative activity of some new thieno[2,3-d] pyrimidin-4(3H)-ones containing 1,2,4-triazole and 1,3,4-thiadiazole moiety, Eur. J. Med. Chem. 86: 676–683.

[16]. Wu, G., Gao, Y., Kang, D., Huang, B., Huo, Z., Liu, H., Poongavanam, V., Zhan, P., Liu, X. (2018). Design, synthesis and biological evaluation of Tacrine 1,2,3-triazole derivatives as potent cholinesterase inhibitors, Med. Chem. Commun 9: 149–159.

[17]. Tikhomirov, A.S., Sinkevich, Y.B., Dezhenkova, L.G., Kaluzhny, D.N., Ilyinsky, N.S., Borshchevskiy, V.I., Schols, D., Shchekotikhin, A.E. (2024). Synthesis and antitumor activity of cyclopentane-fused anthraquinone derivatives, *European Journal of Medicinal Chemistry* doi:

https://doi.org/10.1016/j.ejmech.2023.116103.

[18]. Oyebamiji, A.K., Akintayo, E.T., Akintayo, C.O., Aworinde, H.O., Adekunle, O.D., Akintelu, S.A. (2023). Cyclic RGD-containing peptides: in silico exploration against BCL-X(L). Ukr. Biochem. J. 95(2): 93-105. doi: https://doi.org/10.15407/ubj95.02.093.

[19]. Semire, B., Oyebamiji A. & Odunola, O.A. (2016). Design of (2Z)-2-cyano-2-[2-[(E)-2-[5-[(E)-2-(4-dimethylaminophenyl)vinyl]-2-thienyl]vinyl]pyran-4-ylidene]acetic acid derivatives as D-p-A dye sensitizers in molecular photovoltaics: a density functional theory approach, *Research on Chemical Intermediates*, 42: 4605-4619.

[20]. Muller, Y.A. , Christinger, H.W. , Keyt, B.A., de Vos, A.M. (1997). The crystal structure of vascular endothelial growth factor (VEGF) refined to 1.93 A resolution: multiple copy flexibility and receptor binding. Structure 5: 1325-1338.

[21]. Çevik, U.A., Celik, I., Işık, A., Pillai, R.R., Tallei, T.E., Yadav, R., Özkay, Y., Kaplancıklı, Z.A. (2022). Synthesis, molecular modeling, quantum mechanical calculations and ADME estimation studies of benzimidazole-oxadiazole derivatives as potent antifungal agents. *J. Mol. Struct.* 1252: 132095. https://doi.org/10.1016/j.molstruc.2021.132095

[22]. Ahmad, I., Akand, S.R., Shaikh, M., Pawara, R., Manjula, S.N., Patel, H. (2022). Design, synthesis, in vitro anticancer and antimicrobial evaluation, SAR analysis, molecular docking and dynamic simulation of new pyrazoles, triazoles and pyridazines based isoxazole. *J. Mol. Struct.* 1251: 131972. https://doi.org/10.1016/j.molstruc.2022.133312.

[23]. Halayal, R.Y., Bagewadi, Z.K., Maliger, R.B., Al Jadidi, S., Deshpande, S.H. (2023). Network pharmacology based anti-diabetic attributes of bioactive compounds from Ocimum gratissimum L. through computational approach, Saudi Journal of Biological Sciences, doi:https://doi.org/10.1016/j.sjbs.2023.103766

[24]. Oyebamiji, A.K., Olujinmi, F.E., Akintelu, S.A., Adetuyi, B., Ogunlana, O., Semire, B., Akintayo, E.T., Akintayo, C.O., Babalola, J.O., Olawoye, B.M., Aworinde, J.O. (2024). Predicting the biological activity of selected phytochemicals in Alsophila spinulosa leaves against 4-aminobutyrate-aminotransferase: A potential antiepilepsy agents. *Eclet. Quim*. 49: e-1492.

[25]. Semire, B., Oyebamiji A. and Ahmad, M. (2012). Theoretical Study on structural and electronic properties of 2,5-Bis[4-N,N-Diethylaminostyryl]Thiophene and Its Furan and Pyrole Derivatives using Density Functional Theory (DFT), *Pak. J. Chem.*, 2(4): 166-173.

[26]. Waziri, I., Kelani, M.T., Oyedeji-Amusa, M.O., Oyebamiji, A.K., Coetzee, L-C. C. and Muller, A.J. (2024). Comparative investigation of derivatives of (*E*)-N-((*E*)-3-phenylallylidene)aniline: Synthesis, structural characterization, biological evaluation, density functional theory analysis, and *in silico* molecular docking, Heliyon, 10, e26632. doi: https://doi.org/10.1016/j.heliyon.2024.e26632.

[27]. Abdulazeez, M.O., Oyebamiji, A.K. and Semire, B. (2016). DFT and QSAR study of corrosion inhibition on 3,5-di-substituted pyrazole derivatives with heteroatom on position one, *Lebanese Science Journal*, 17(2): 217-232.

[28]. Pegu, D., Deb, J., Alsenoy, C.V. & Sarkar, U. (2017). Theoretical Investigation of Electronic, Vibrational and Nonlinear Optical Properties of 4-fluoro-4- hydroxybenzophenone, Spectroscopy Letters.

[29]. Migahed, M. A., Zaki, E. G., Shaban, M. M. (2016). Corrosion control in oil wells tubing steel during matrix acidizing operations. *The Royal Society of Chemistry Advances*, 6: 71384-71396.

[30]. Oyebamiji, A.K., Fadare, O.A., and Semire, B. (2020). Hybrid-based drug design of 1,2,3-triazolepyrimidine-hybrid derivatives: Efficient inhibiting agents of mesenchymal–epithelial transition factor reducing gastric cancer cell growth. Journal of Chemical Research, 44(5-6) 277–280.

[31]. Ruddarraju, RR., Murugulla, AC., Kotla, R., Tirumalasetty, MCB., Wudayagiri, R., Donthabakthuni, S., Maroju, R. (2016). Design, synthesis, anticancer activity and docking studies of theophylline containing 1,2,3-triazoles with variant amide derivatives. Medchemcomm. 8(1): 176-183. doi: 10.1039/c6md00479b.

[32]. Morakinyo, A.E., **Oyebamiji**, **A.K.,** Ayoola, M., Chukwuetoo, C.C., Oyedapo O.O. (2024). Antioxidant and Anti-inflammatory Activities of Methanolic Pulp Residue Extract of African Star Apple (*Chrysophyllum albidum*). Letters in Applied Bionanoscience, 13(1): 1-9.

[33]. Oyebamiji, AK., Olujinmi, F.E., Akintelu, S.A., Adetuyi, B., Ogunlana, O., Semire, B., Akintayo, E.T., Akintayo, C.O., Babalola, J.O., Olawoye, B.M., Aworinde, J.O. (2024). Predicting the biological activity of selected phytochemicals in Alsophila spinulosa

leaves against 4-aminobutyrate-aminotransferase: A potential antiepilepsy agents. *Eclet. Quim*. 49: e-1492.

[34]. Kalantzi, L., Goumas, K., Kalioras, V., Abrahamsson, B., Dressman, J.B., Reppas, C. (2006). Characterization of the human upper gastrointestinal contents under conditions simulating bioavailability/bioequivalence studies, Pharm. Res. 23 (1): 165–176.

[35]. Speciale, A., Muscar_a, C., Molonia, M.S., Cimino, F., Saija, A., Giofr_e, S.V. (2021). Silibinin as potential tool against SARS-Cov-2: in silico spike receptor-binding domain and main protease molecular docking analysis, and in vitro endothelial protective effects, Phytother Res.

[36]. Adeleke, M., Adegoke A. (2020). In-Silico Studies and Property Model to Investigate The Binding Effect of Selected Ligands on HIV Integrase. *BASRA J. Sci. 38*(2), 174–197. https://doi.org/10.29072/basjs.202023.

[37]. Adegoke A.B, Oyelowo T.M, Sanusi J.D. (2020). Computational Studies of 1,2,3-Triazoles Derivatives against Yellow Fever Virus: DFT Based. *Eur. Mod. Stud. J. 4* (1), 94–103.

[38]. Adegoke A. B., Abeedha T. K., Adepoju, R.A. A. (2020). Molecular Dynamic (MD) Simulation and Modeling the Bio-Molecular Structure of Human UDP Glucose -6-Dehydrogenase Isoform 1 (hUGDH) Related to Prostate Cancer. *BASRA J. Sci. 38* (3), 448–466. https://doi.org/10.29072/basjs.202036.

[39]. Adegoke A., Azeez, G., Lawal, A., Imran M. (2021). Theoretical Studies of 1, 2, 3-Triazole and Isoxazole-Linked Pyrazole Hybrids as Antibacterial Agents: An Approach of Docking and Density Functional Theory. *Adv. J. Chem.-Sect. B*.https://doi.org/10.22034/ajcb.2021.265760.1075.